Influence of domain wall structure on pinning characteristics with self-induced anisotropy

H. Asada[a] and Y. Wasada
Department of Symbiotic Environmental Systems Engineering, Graduate School of Science and Engineering, Yamaguchi University, 2-16-1 Tokiwadai, Ube 755-8611, Japan

J. Yamasaki and M. Takezawa
Department of Electrical Engineering, Faculty of Engineering, Kyushu Institute of Technology, 1-1 Sensui-cho, Tobata-ku, Kitakyushu 804-8550, Japan

T. Koyanagi
Department of Symbiotic Environmental Systems Engineering, Graduate School of Science and Engineering, Yamaguchi University, 2-16-1 Tokiwadai, Ube 755-8611, Japan

(Presented on 13 November 2002)

Wall pinning effects with self-induced spatially varying uniaxial anisotropy in various thick films have been studied using micromagnetic simulation based on the Landau–Lifshitz–Gilbert equation. In the simulation, the discretization region is in the cross section normal to the film plane. It is clarified that the wall structure is strongly related to pinning characteristics. Depinning fields of the wall having a flux-closure asymmetric vortex (C-shaped wall) are different in the wall movement directions due to the asymmetric wall structure. On the other hand, depinning fields of the wall with two vortices (S-shaped wall) which have a symmetric structure do not depend on the wall movement direction. Depinning fields for the S-shaped wall are different from both depinning fields for the C-shaped wall. © *2003 American Institute of Physics.* [DOI: 10.1063/1.1560703]

I. INTRODUCTION

It is well known that amorphous ribbons annealed in a demagnetized state exhibit magnetization reversal with large Barkhausen discontinuities due to the domain wall pinning. The mechanism for the wall pinning is self-induced anisotropy during annealing by the domain wall itself.[1] Kerr microscope observation revealed the pinned wall broadening and magnetization reversal process in a Perminvar-type loop.[2,3] Theoretical analysis and micromagnetic simulation on self-induced anisotropy effects on domain wall within a one-dimensional approximation was also performed.[4,5] However, the domain wall behaviors with self-induced anisotropy, which plays an important role for magnetic properties, has not been clarified well since the domain wall contains Néel caps and Bloch wall in thin films.[6] Magnetization within the wall, therefore, rotates along the film thickness direction as well as the direction normal to the wall plane. We have done the micromagnetic simulation based on the Landau–Lifshitz–Gilbert (LLG) equation assuming the cross section normal to the film plane and studied on domain wall behaviors such as wall broadening and wall pinning with spatially varying uniaxial anisotropy.[7] In this article, we investigate the influence of domain wall structures on wall pinning characteristics with spatially varying uniaxial anisotropy in various thick films.

II. SIMULATION MODEL

Numerical simulations were carried out by integrating the LLG equation.[8] The cross section normal to the film plane was discretized into a two-dimensional array. Self-induced anisotropy was modeled as follows: first, with the uniform easy axis set normal to the calculation region, the domain wall profile was calculated. Next, after relaxation, with the easy axis direction set to be the same as the magnetization direction, the domain wall profile was recalculated. This procedure was iterated when wall broadening was investigated. The material parameters used in the simulation were as follows: saturation induction $4\pi M_s = 8000$ Gauss, uniaxial anisotropy constant $K_u = 3800$ erg/cm^3, exchange constant $A = 10^{-6}$ erg/cm, and gyromagnetic ratio $\gamma = 1.76 \times 10^7$ erg/(s Oe). The damping constant $\alpha = 1.0$ was chosen to speed up the computation. The grid element spacings were 50 Å for the film thickness $h = 0.15$ μm, 100 Å for $h = 0.3$ and 0.5 μm, and 150 Å for $h = 0.8$ μm, respectively.

III. RESULTS AND DISCUSSION

Figure 1 shows magnetic configuration and energy curves of a domain wall part of the calculation region, hav-

[a]Author to whom correspondence should be addressed; electronic mail: asada@aem.eee.yamaguchi-u.ac.jp

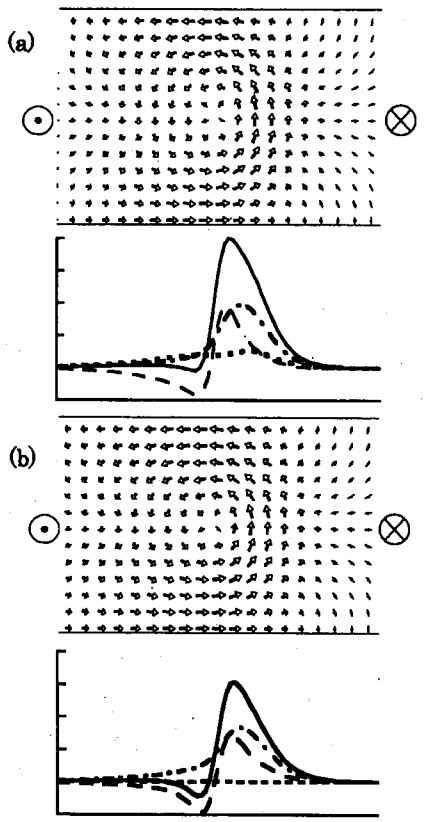

FIG. 1. Simulation results of magnetization configuration and wall energy curve (solid line) for an asymmetric Bloch wall (C-shaped wall) in a 0.8 μm thick film (a) easy axis along x; (b) with the easy axis profile set to the domain wall profile. The wall energy components of anisotropy (dotted), demagnetization (dashed), and exchange (dotted–dashed) are also indicated.

ing a flux-closure asymmetric vortex (C-shaped wall), in a 0.8 μm thick film (a) with the uniform easy axis set normal to the calculation region (x-direction); (b) with the easy axis profile set to the domain wall profile. The arrows in the figures represent the magnetization directions for every fourth (4×4) grid element. Energies are averaged through the film thickness and normalized by the peak of the wall energy in Fig. 1(a). The magnetization rotation in Fig. 1(b) becomes more gradual not only along the direction normal to the wall plane (y-direction) but also along the film thickness direction (z-direction). Reflecting the magnetization configuration, the wall energy curves show an asymmetric shape. The slope of the energy curves are steeper at the left side of the Bloch wall in the center of film thickness, that is, the vortex side. Comparing the wall energy components in Figs. 1(a) and 1(b), the anisotropy energy drastically dropped, which occurred at the first iteration of an easy axis profile set to the domain wall profile. The exchange energy also decreased monotonically with the repeated iteration, while the demagnetization energy variation was small.[7] Positive and negative magnetic fields were applied along the magnetic domain to investigate the pinning characteristics. When the positive magnetic fields were applied, the wall moved to the right-hand side of Fig. 1. The time transient of the orthogonal component of an effective field is used for determining the depinning field.[9] Depinning fields as a function of film thickness are shown in Fig. 2. It was confirmed that, in the 0.15

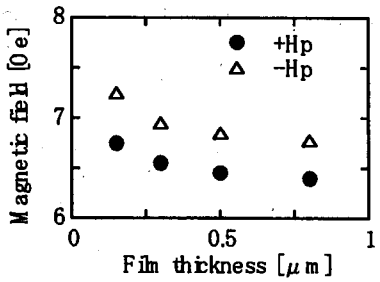

FIG. 2. Depinning fields of the C-shaped wall as a function of film thickness for positive and negative magnetic fields.

μm thick film, depinning fields for $\alpha=1.0$ were the same as those for $\alpha=0.1$. As shown in Fig. 2, depinning fields are different in the wall movement direction for various thick films due to the asymmetric wall structure, which causes the asymmetric energy profile as shown in Fig. 1. The depinning fields for both the positive and negative applied fields decrease with increasing film thickness and tend to saturate. The depinning fields for $h=0.8$ μm are 0.54 H_k and 0.57 H_k ($H_k=2K_u/M_s$) for the positive and negative applied fields, respectively. These values are similar to the numerically obtained depinning field of 0.55 H_k within the one-dimensional approximation.[5] On the other hand, the difference of depinning fields in wall movement directions are almost the same for the various thick films.

Next, we investigated the depinning field for the different types of wall which has two vortices (S-shaped wall). Figure 3 shows the magnetic configuration (every 4×4 grid elements) and normalized energy curves of a domain wall part of calculation region, having an S-shaped wall, in a 0.15 μm thick film with the easy axis profile set to the domain wall profile. As shown in the figure, the wall energy curve for the S-shaped wall shows the symmetric shape having two peaks near each vortex where the magnetization rapidly rotates along the y and z directions. Simulated wall energies of the S-shaped wall (1.7 erg/cm^2 for $h=0.15$ μm and 0.45 erg/cm^2 for $h=0.8$ μm) is higher than those for the C-shaped wall (1.3 erg/cm^2 for $h=0.15$ μm and 0.32 erg/cm^2 for $h=0.8$ μm). The depinning fields are also examined by applying positive and negative magnetic fields. Figure 4 shows depinning fields of the S-shaped wall as a function of film thickness. The depinning field decreases

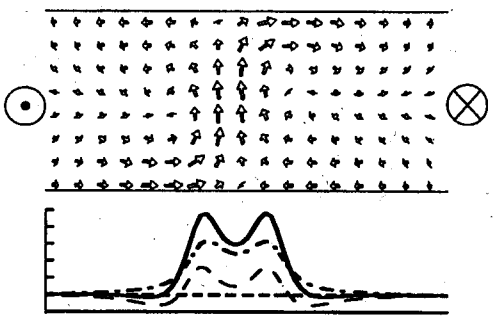

FIG. 3. Magnetization configuration and wall energy curve for an S-shaped wall in a 0.15 μm thick film. The easy axis profile is set to the wall profile. The wall energy components of anisotropy (dotted), demagnetization (dashed), and exchange (dotted–dashed) are also indicated.

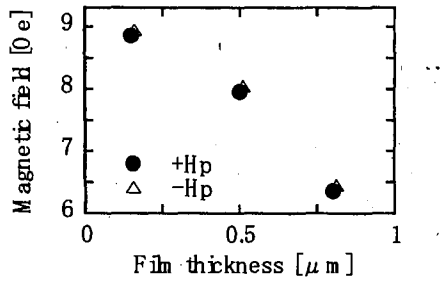

FIG. 4. Depinning fields of the S-shaped wall as a function of film thickness for positive and negative magnetic fields.

with increasing film thickness. In contrast to the C-shaped wall, the depinning fields for the S-shaped wall do not depend on the wall movement direction due to the symmetric structure. It is also found that the depinning field for the S-shaped wall is different from both depinning fields for the C-shaped wall.

Finally, pinning effects of spatially varying uniaxial anisotropy on domain walls having different kinds of profiles from an easy axis profile as shown in Fig. 5 are investigated. The easy axis direction of spatially varying uniaxial anisotropy [Fig. 5(a)] is set to the same kind of C-shaped wall profile as Fig. 1. The assumed film thickness is 0.15 μm. In this simulation, the domain walls having the Bloch wall in which the magnetization rotates in the same direction of the easy axis profile are chosen. First, the interaction for the

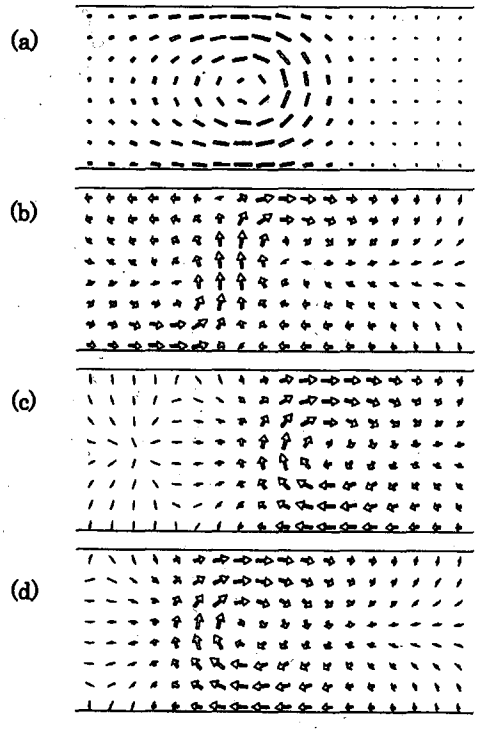

FIG. 5. (a) Easy axis directions and magnetization configurations for (b) S-shaped and (c) and (d) C-shaped walls having different kinds of profiles from an easy axis profile.

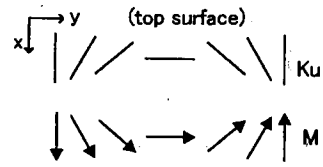

FIG. 6. Schematic drawing of easy axis [Fig. 5(a)] and magnetization of the C-shaped wall [Figs. 5(c) and 5(d)] at the top of the film surface.

S-shaped wall is examined. The simulated magnetic configuration (every 4×4 grid elements) of the domain wall part without the applied field is indicated in Fig. 5(b). This type of domain wall would correspond to the experimentally observed "unstable wall" having the black-and-white contrast using the Kerr magneto-optical effect,[2] which means that the domain wall at the film surface consists of the two magnetization regions having $+y$ and $-y$ components. Obviously, the wall energy for the S-shaped wall is higher than that for the C-shaped wall energy with the same spatially varying uniaxial anisotropy. The depinning fields are 5.0 Oe for both the positive and negative applied fields and the dependence of the wall movement directions on depinning fields is not observed. Second, the interaction for different types of C-shaped walls having the Néel caps where magnetization rotates in the opposite direction of the easy axis profile as depicted schematically in Fig. 6 is investigated. In this case, there are two pinning sites as shown in Figs. 5(c) and 5(d). The pinning site as Fig. 5(d) is more stable compared to Fig. 5(c). The obtained depinning fields of 3.3 Oe for the positive applied field and 1.1 Oe for the negative applied fields are considerably smaller.

IV. CONCLUSIONS

Numerical simulation shows that the wall structure is strongly related to pinning characteristics with self-induced spatially varying uniaxial anisotropy. Different wall structures yield different pinning characteristics due to the different self-induced anisotropy. Depinning fields of the C-shaped wall are different in the wall movement directions due to the asymmetric wall structure, while depinning fields of the S-shaped wall do not depend on the wall movement direction.

[1] H. Fujimori, H. Yoshimoto, T. Masumoto, and T. Mitera, J. Appl. Phys. **52**, 1893 (1981).
[2] R. Schafer, W. K. Ho, J. Yamasaki, A. Hubert, and F. B. Humphrey, IEEE Trans. Magn. **27**, 3678 (1991).
[3] J. Yamasaki, T. Chuman, M. Yagi, and M. Yamaoka, IEEE Trans. Magn. **33**, 3775 (1997).
[4] C. Aroca, P. Sanchez, and E. Lopez, Phys. Rev. B **34**, 490 (1986).
[5] B. B. Pant, K. Matsuyama, J. Yamasaki, and F. B. Humphrey, Jpn. J. Appl. Phys., Part 1 **34**, 4779 (1995).
[6] A. Hubert, Phys. Status Solidi **32**, 159 (1969).
[7] H. Asada, Y. Wasada, J. Yamasaki, M. Takezawa, and T. Koyanagi, J. Magn. Soc. Jpn. **26**, 392 (2002).
[8] S. Konishi, K. Matsuyama, N. Yoshimatsu, and K. Sakai, IEEE Trans. Magn. **24**, 3036 (1988).
[9] H. Asada, K. Matsuyama, M. Gamachi, and K. Taniguchi, J. Appl. Phys. **75**, 6089 (1994).